



CrossMark
click for updates

Cite this: DOI: 10.1039/c5lc00816f

Microfluidic device for DNA amplification of single cancer cells isolated from whole blood by self-seeding microwells†

Yoonsun Yang,^{‡a} Hoon Suk Rho,^{‡b} Michiel Stevens,^c Arjan G. J. Tibbe,^c Han Gardeniers^b and Leon W. M. M. Terstappen^{*a}

Self-seeding microwell chips can sort single cells into 6400 wells based on cell size and their identity verified by immunofluorescence staining. Here, we developed a microfluidic device in which these single cells can be placed, lysed and their DNA amplified for further interrogation. Whole blood spiked with MCF7 tumor cells was passed through the microwell chips after leukocyte depletion and 37% of the MCF7 cells were identified by epithelial cell adhesion molecule (EpcAM) staining in the microwells. Identified single cells were punched into the reaction chamber of the microfluidic device and reagents for cell lysis and DNA amplification introduced sequentially by peristaltic pumping of micro-valves. On-chip lysis and amplification was performed in 8 parallel chambers yielding a 10 000 fold amplification of DNA. Accessibility of the sample through the reaction chamber allowed for easy retrieval and interrogation of target-specific genes to characterize the tumor cells.

Received 12th July 2015,
Accepted 4th September 2015

DOI: 10.1039/c5lc00816f

www.rsc.org/loc

Introduction

Genetic characterization of tumor cells is crucial to determine the aggressiveness of the disease, and determine which treatments are likely to be effective. Cells within a tumor are however heterogeneous and alterations during the course of the disease give rise to resistance to therapy and poses a tremendous challenge. These alterations frequently only occur in subgroup of cells.^{1,2} Therefore genetic analysis at the population level will give the averaged information and certain alterations can be missed either by the low frequency of the sub-population among the tumor cells or the presence of non tumor cells. Especially efficiency of targeted therapy can be guided based on the expression of target genes. For example, patients whose tumor cells have her-2 gene amplification will likely respond to Trastuzumab.^{3,4} The expression of her-2 can however vary between the tumor cells and without assessment of the expression at the single cell level the information will

not be available.⁵ This urges the need to investigate tumors at the single cell level and preferably at each time therapeutic intervention is needed.⁶ The presence of circulating tumor cells (CTC) provides a great opportunity to obtain a “real time biopsy” of the tumor.^{7–10} The load of CTC is directly associated with the prognosis of the patient¹¹ and in most cases their frequency is low and no more than 1–10 CTC in a 7.5 ml blood sample are present among 10⁷ white blood cells and 10¹¹ red blood cells.¹²

Several methods have been introduced to enrich, identify, isolate and characterize these rare cells.^{13–18} However, following an enrichment procedure of CTC from blood, the identification, isolation and manipulation of single cells for further analysis without loss of cells remains challenging. Microfluidic devices are highly attractive to manipulate individual cells. Various microfluidic systems have shown the capability to capture single cells using hydrodynamic flow, surface modification for antibody binding, optical detection, magnetic separation, or electrical fields.^{19–23} However, not many devices showed the integration of genetic analysis of individual cells on the same chip after cell capture. The limited DNA content of a single cell makes it necessary to amplify the DNA before a detailed genetic characterization of single cells can be obtained. On-chip single cell amplification of DNA has the advantage of a reduced reagent volume resulting in a reduction of cost and can improve the quality of amplified DNAs.²⁴ Microfluidic devices using integrated micro-valves were used to capture up to hundreds of single cells individually and process the content of each individual cell by lysis,

^a Medical Cell BioPhysics Group, MIRA Institute for Biomedical Technology and Technical Medicine, University of Twente, The Netherlands. E-mail: l.w.m.m.terstappen@utwente.nl

^b Mesoscale Chemical Systems Group, MESA+ Institute for Nanotechnology, University of Twente, The Netherlands

^c VyCAP, B.V., Deventer, The Netherlands

† Electronic supplementary information (ESI) available: Supplementary movie1 shows peristaltic pumping of color dye to the reaction chamber. Supplementary information in PDF file shows the detailed experimental procedure with the process time (Table S1(S1)) and description about the leukocyte depletion procedure (ESI 2(S2)). See DOI: 10.1039/c5lc00816f

‡ Both authors contributed equally.

DNA amplification and polymerase chain reaction (PCR) or including reverse transcription (RT) and RT-PCR.^{23,25,26} They however do not provide a solution for the capture and analysis of the content of only the cells of interest present in whole blood.

Recently, our group developed a single cell isolation method based on self-seeding microwell chips.²⁷ After deposition of a cell solution on the microwell chip single cells are contained in the microwells for further single cell analysis.

Here we make use of this technology and introduce a novel approach to isolate and interrogate individual CTC. Even though erythrocytes and majority of leukocytes can pass through the hole at the bottom of the microwell, the number of leukocytes are too high in whole blood. Therefore, we depleted leukocytes from whole blood to fit the capacity of the self-seeding microwells after immunostaining of tumor cells. The cell suspension is placed on a microwell chip, EpCAM+ cells are “punched” into a microfluidic device in which the DNA is amplified for genetic characterization of individual tumor cells.

Materials and method

Chip design and fabrication

The microfluidic devices were fabricated by multilayer soft lithography.^{28,29} The mask designs were prepared with CleWin software (WieWeb software, Hengelo, The Netherlands) and printed on a 5" soda lime glass by a mask generator LBP Heidelberg DWL200 (Heidelberg Instruments Mikrotechnik GmbH). The master molds were fabricated by a photoresist-based photolithographic technique. Positive photoresist (AZ 40 XT, MicroChem Corp.) was spin-coated onto a 4" silicon wafer, and patterned using photolithography. For reliable operations of the micro-valves, the cross-sectional shape of microchannels in the fluidic channels was rounded by heating the mold at 140 °C for 1 min after development. The fluidic layer was produced by pouring uncured polydimethylsiloxane (PDMS, GE RTV 615, elastomer:cross-linker = 5:1) onto the mold to achieve a thickness of 7 ± 0.5 mm. The control layer was made by spin-coating uncured PDMS (elastomer:cross-linker = 20:1) onto the master mold at 2500 rpm for 1 min. The resulting thickness of the control layer was 25 ± 2 μm. The fluidic and control layers were cured for 45 min and 30 min, respectively, at 80 °C. The fluidic layer was peeled off from the mold and holes for inlets and outlets were punched with a 25-gauge punch (Syneo Co., Angleton, TX, USA). Subsequently, the fluidic layer was aligned over the control layer using the alignment marks on both layers under a stereomicroscope and the aligned layers were bonded by baking at 80 °C for 60 min. The bonded layers were peeled off from the mold, and holes for control ports were punched.

For the bottom substrate with open-wells, 8 holes with 1 mm diameters were drilled through the glass slides (Fisher Scientific, Landsmeer, The Netherlands) in advance. Uncured PDMS mixture (elastomer:cross-linker = 20:1) was dissolved

in hexane at a 1:4 weight ratio and spun onto the glass substrate at 3800 rpm for 2 min. Then, the glass substrate was baked at 80 °C for 20 min. The multi-layer PDMS device was aligned on a glass slide and kept in the oven at 80 °C for 12 hours to enhance adhesion. The device was cleaned by flowing 70% ethanol. A sterile sharp needle (BD, Fraga, Spain) was used to make a hole in the membrane and connect the fluidic channel to the reaction chamber under a stereomicroscope. To avoid undesired adsorption of DNA, the fluidic channels were coated with 1% bovine serum albumin (BSA) solution (Sigma-Aldrich Chemie B.V., The Netherlands) for 5 min, followed by drying with air for 5 min.

Self-seeding microwell chips. The procedure for making self-seeding microwell chips is described in detail elsewhere.²⁷ Each plate contains 6400 microwells in an effective area of 8×8 mm². Each well has a diameter of 70 ± 2 μm and a depth of 360 ± 10 μm resulting in a well volume of 1.4 nL. The bottom of the well is a thin, optically transparent, silicon nitride (SiN) membrane with a thickness of 1 μm. The center of the bottom contains a single pore with a diameter of 5 μm.

Sample preparation

The research does not fall within the scope of the Dutch Medical Research Involving Human Subjects Act. Blood was collected in a 6 ml blood collection tube containing ethylenediaminetetraacetic acid (EDTA) as anticoagulant (BD, Franklin Lakes, USA) from anonymized healthy volunteers at the University of Twente. Informed consent was obtained from all volunteers and the used blood collection procedure was approved by the local Medical Ethical Committee. The research complies with all applicable laws and institutional guidelines. MCF-7 (human breast adenocarcinoma cell line, ATCC HTB-22TM) cells were cultured in Dulbecco's Modified Eagle Medium (Sigma Aldrich, Zwijndrecht, The Netherlands), supplemented with 10% Fetal Bovine Serum (Sigma Aldrich), 2 mM L-Glutamin (Sigma Aldrich), 1% penicillin-streptomycin (Sigma Aldrich) at 37 °C in 5% CO₂ atmosphere. Cells were detached using 0.05% of Trypsin/EDTA (Gibco, Paisely, UK). Aliquots of 1 ml of blood were spiked with 1000 MCF-7 cells and leukocytes were depleted from the blood using the RosetteSep CTC enrichment kit according to the procedure recommended by the manufacturer (Stemcell technologies, Vancouver, Canada). The detailed procedure is described in ESI†2(S2). After depletion, the cell suspension was stained with Hoechst 33342 (Invitrogen, Breda, The Netherlands) and phycoerythrin(PE) conjugated anti-EpCAM(Sigma Aldrich) for 30 min at 37 °C. Cells were washed and re-suspended in 4 ml of 1× phosphate buffered saline (PBS) containing 1% BSA.

Cell filtration, scanning and isolation

A self-seeding microwell chip (VyCAP, Deventer, The Netherlands) was degassed in 1× PBS containing 0.1% Tween-20 for 30 min under vacuum. A microwell chip was inserted onto

the disposable filtration unit and placed on a filtration system (VyCAP).

The 4 ml cell suspension was carefully loaded onto the disposable filtration unit and filtrated using a pressure of -10 mbar. The microwell chip was placed on an inverted fluorescence microscope equipped with computer controlled X, Y, Z stages for scanning the microwell chip and an additional stage to move the wells of interest to a needle that allowed to punch the bottom of the wells into the microfluidic device as described in detail elsewhere.²⁷ A custom-made LabVIEW (National Instruments Co.) program was used to control the microscope in order to scan the complete area of the microwell chip with a $10\times$ numerical aperture (NA) 0.45 objective using filter cubes for Hoechst and PE. The program was also used to analyse the images and identify and count the different cell types and select the wells that contained cells of interest. The scanned microwell chip was dried under the flow hood and left overnight. We selected the cells of interest based on fluorescence staining and punched the bottom of the well containing the desired cells into the reaction chamber of the microfluidic device. The needle was aligned in the middle of the reaction chamber before punching and isolated cells were observed under a fluorescence microscope.

DNA amplification

Repli-g single cell kit (Qiagen, Venlo, The Netherlands) was used for DNA amplification. The lysis buffer was prepared according to the protocol provided with the kit. After pumping the lysis buffer into the 8 reaction chambers, the device was placed in a water bath for 10 min and the temperature was set at 65 °C. Stop solutions and amplification mixture ($2\times$ polymerase was used) were sequentially pumped into the reaction chambers. After 16 h of amplification at 30 °C, $1\times$ Tris-EDTA buffer containing 0.2% Tween-20 was pushed into the individual reaction chambers and samples were collected using a pipette from the open-structure of the reaction chambers. This was followed by an inactivation step at 65 °C for 10 min after which the samples were transferred to a 96 well PCR plate.

Purification, quantification and qPCR

Agencourt Ampure XP beads (Beckman Coulter Inc., Woerden, The Netherlands) were used to purify amplified samples. After purification dsDNA was quantified using Qubit 2.0 Fluorometer and Qubit dsDNA HS Assay Kit (Invitrogen). Real-time SYBR green quantitative polymerase chain reaction (qPCR) was used for amplifying target-specific DNA. Primers were designed to target small subunits of ERBB2 (17q12), CCND1 (11q13), MyC (8q24.21), PRMT2 (21q22.3), URB2 (1q42.13), P53 (17p13.1), TRAM1 (8q13.3), and PAK1 (11q13-q14) and were used at a concentration of 500 nM.

Result and discussion

We designed and fabricated a microfluidic device to isolate single tumor cells from leukocyte depleted whole blood followed by on-chip cell lysis and DNA amplification as illustrated in Fig. 1. In Fig. 1(A) the deposition of single cells in microwells is shown, Fig. 1(B) shows the identification of DNA+, EpCAM+ cancer cells, Fig. 1(C) shows the isolation of single cancer cells into the open-reaction chamber of the microfluidic device by punching and Fig. 1(D) shows the lysis of the cells isolated and amplification of DNA in the reaction chamber. Fig. 1(E) shows the validation process using purification and qPCR. The detailed procedure including process time is available in Table S1†(S1).

Device design

The device was designed to integrate self-seeding microwell chips and on-chip DNA amplification by introduction of open-chambers to collect the cells and micro-valves to add reagents into the chambers. Open micro-chambers made onto a PDMS layer have been introduced recently into microfluidic platforms for the delivery of cell solutions.³⁰ In general a thickness of a few millimeters has been chosen for PDMS devices because of the ease of use and convenience in the fabrication of the devices and the connection to the fluidic tubing. However, the deformability of PDMS makes it challenging to achieve confined well-structures needed for accurate punching of the cells into the chambers. Hence we drilled holes with a diameter of 1 mm through a microscope glass slide to form the reaction chambers. Fig. 2(A) shows the top view and the side view of the device. The device consists of three layers, a glass substrate layer (gray), a control PDMS layer (red), and a fluidic PDMS layer (blue). Below the glass chambers, a thin PDMS membrane (pink) is present at the top of the fluidic layer (blue). To connect the fluidic channel to the reaction chamber a sterile sharp needle was used to make a hole in the thin PDMS membrane (brown). A microscope image of the actual device containing 8 reaction chambers is shown in Fig. 2(B). Five inlets controlled by micro-valves for different reagents were designed into the device to perform the BSA pre-coating, the lysis, the neutralization and the DNA amplification. In front of the inlets three valves were placed in a row and actuated in a certain sequence to perform the peristaltic pumping.³¹ Multiplexer valves were placed in front of the channels connected to the 8 chambers to add reagents to each chamber individually.³² Color dyes were introduced in 4 inlets except the inlet for air-drying to visualize and characterize the device. Fig. 2(B) shows an image of 4 different color dyes that were pumped into 8 individual chambers to demonstrate reagent loading using micro-valve manipulation.

Peristaltic pumping

Fig. 3(A) shows the dimensions of the micro-valves used for peristaltic pumping, Fig. 3(B) shows the sequence of

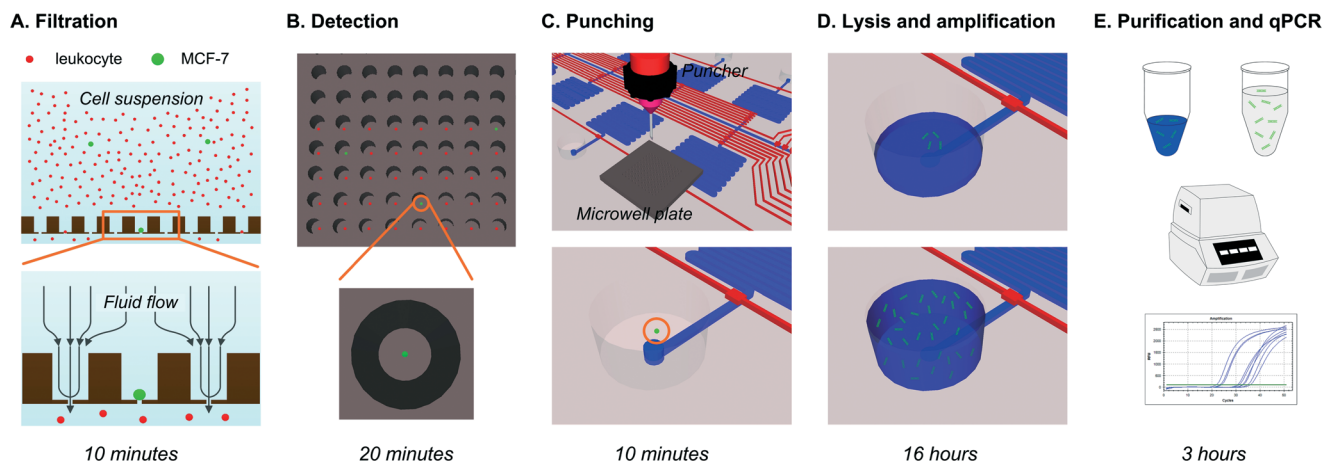


Fig. 1 Experimental scheme (A) filtration of 1 ml of leukocyte depleted blood through a microwell chip (B) detection of cells of interest (MCF-7) based on fluorescence staining (C) isolation of cells by punching the bottom of the well containing MCF-7 cells into the reaction chamber (D) lysis and DNA amplification in a reaction chamber of the microfluidic device integrated with micro-valves to pass fluids and introduce reagents by peristaltic pumping. (E) DNA purification and qPCR analysis after retrieving amplified DNA from the reaction chamber.

operation, and Fig. 3(C) shows the pumping rates at various frequencies. In Fig. 3(B), the closed valves are represented as (1) and the open valves are represented as (0). Pressurizing in the sequence pattern, (0 0 1), (0 1 0), (1 0 0), delivered a constant volume of the solution across the pumping valves. To evaluate the pumping rates we introduced blue color dye in one of the inlets. A real-time movie was recorded during the peristaltic pumping and the volume of solution moved forward per second could be calculated. Below 10 Hz frequency of operating sequence cycle pumping rates increase with operation speed. The maximum pumping rate was obtained at 10 Hz and is approximately 2.5 nl s^{-1} . Peristaltic pumping added solutions gently to the reaction chamber from the center of the chamber with precise control of the fluid (Supplementary movie). Addition of the reagents sequentially to the reaction chambers eliminated a transfer step thereby keeping the loss of DNA to a minimum.

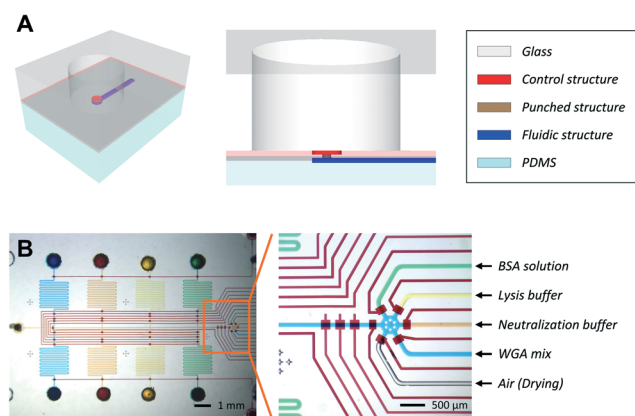


Fig. 2 Design of the device (A) illustration of top and side views of the microfluidic device (B) photo of the actual microfluidic device with color dyes to visualize the microchannel network.

Sample preparation and cell isolation

To demonstrate rare cell isolation from blood sample, we spiked MCF-7 cells into 1 ml of blood from healthy donors. After depletion of leukocytes the blood was stained with Hoechst and a PE labeled monoclonal antibody recognizing EpCAM present on cells of epithelial origin. After the cells were resuspended in 4 ml of PBS containing 1% BSA, the suspension was placed on the microwell chip. After filtration under -10 mbar , fluorescence images of Hoechst and PE and reflection images were taken covering the complete area of the microwells. Fig. 4 shows microscope images of the cells. Fig. 4(A) shows a section of the microwells with 5 MCF-7 cells (blue Hoechst+, green EpCAM+) indicated with green arrows and 2 leukocytes (blue Hoechst+, green EpCAM-) indicated with red arrows. Fig. 4(B) shows a higher magnification of two wells one with a MCF-7 cell (green arrow) and one with a leukocyte (red arrow). Fig. 4(C) shows one well containing one tumor cell before punching and Fig. 4(D) shows the same well after punching in which the bottom of the well is no longer present. Fig. 4(E) and (F) show an isolated MCF-7 cell in the microfluidic reaction chamber. The number of

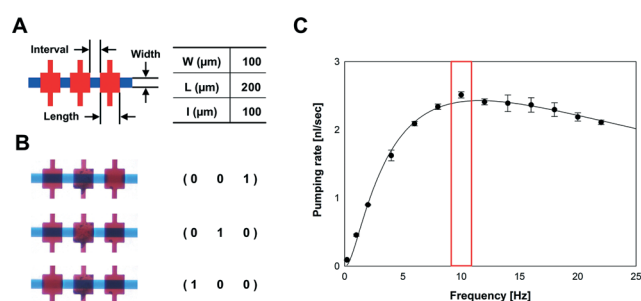


Fig. 3 Peristaltic pumping (A) dimension of micro-valves for the peristaltic pump (B) sequence of operation (C) pumping rates at various frequencies.

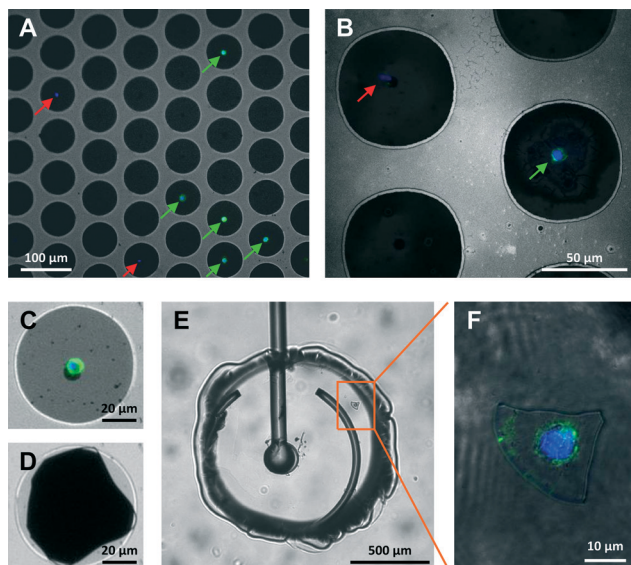


Fig. 4 Single cell isolation using self-seeding microwells. Hoechst and anti-EpCAM PE are represented as blue and green, respectively. (A) Microscope image of 5 MCF-7 cells (green arrow) and 2 leukocytes (red arrow) in a section of the 6400 self-seeding microwell chip. (B) Magnified image of single leukocyte and single MCF-7 cell in microwells. MCF-7 cell in a microwell before (C) and after (D) punching. Isolated single MCF-7 cell in a reaction chamber of the microfluidic device (E and F).

microwells in the chip is 6400 and can result in 6400 single cells when all microwells are filled.²⁷ The 5 μm size of the hole in the bottom of the well was chosen such that all erythrocytes and platelets pass as well as the majority of leukocytes.^{14,33} The larger and stiffer tumor cells will block the pore in the bottom resulting in a stop of the flow in the microwell and cells will be directed to adjacent microwells. In previous experiments 1 cm^2 microsieves containing 118 000 pores were used to filter 7.5 ml of blood.³⁴ In this blood volume $\sim 4 \times 10^7$ leukocytes were present and this number of pores was just sufficient to pass this blood volume without blocking the microsieve. To use the microwell chip for passing this blood volume either the number of microwells have to be increased or the number of the leukocytes decreased. To demonstrate the potential of this approach we used the latter approach and depleted leukocytes from whole blood. In three experiments ~ 1000 MCF-7 cells were spiked into whole blood and after leukocytes depletion the cells were stained and passed through the microwell chip. Table 1

Table 1 Enrichment of MCF-7 cells in 1 ml of whole blood

	# Leukocytes		# MCF7	
	Before depletion	In microwells	Before depletion	In microwells
1	4.3×10^6	179	1000	396
2	4.3×10^6	325	1000	419
3	6.7×10^6	518	1000	307

shows the number of leukocytes and MCF-7 cells in 1 ml whole blood and the number of occupied wells after enrichment.

After examination of the microwell chips by fluorescence microscopy: 396 (39.6%), 419 (41.9%) and 307 (30.7%) MCF-7 cells were detected. The average recovery rate of 37% is lower than the 65% recovery rate we reported using microsieves in our previous work.¹⁴ Difference may be explained by the cup structure around the 5 μm pores, the presence of only 6400 pores *versus* 115 000 pores, or the leukocyte depletion, which also includes a density separation. Further investigation will be needed to identify the cause and increase the recovery. The majority of the cell loss can be attributed to the depletion and staining protocol that includes several washes. Future improvements in the tumor cell recovery can be achieved by the elimination of the density separation in the leukocyte depletion protocol and elimination of the washing steps by for example staining in the microwells. Integration of the microwell chip with larger numbers of wells or a microfluidic device designed for blood cell depletion in previous step might be able to improve recovery rate and reduce the cost of time and reagent for depletion process. In these experiments 179 (3%), 325 (5%), and 518 (8%) of the 6400 wells were occupied with EpCAM⁺ cells resulting in an occupancy of the microwells of respectively 8.98%, 11.63%, and 12.89%. 87% of microwells were not occupied after filtrating 1 ml of leukocyte depleted whole blood and the capacity should thus be sufficient to increase the blood volume to 7.5 ml (CellSearch standard).

For on-chip DNA amplification, MCF-7 cells were isolated from the microwells using a needle with a 50 μm diameter. After identification of a microwell containing a MCF-7 cell, the automated stage positioned the chosen microwell under the needle. The needle was aligned to the center of the open-chamber of the microfluidic device and the needle was moved down to punch the bottom of the micro-well including the MCF-7 cell into the open-chamber. Isolated cells in a reaction chamber of the microfluidic device were observed under a fluorescence microscope to evaluate the number and type of cells. Observation of cells after isolation in the microfluidic chamber is much easier as compared to cells in the wells of a PCR plate because of the transparency of the material and the lower depth of the chamber. Duplicates of 25, 5 cells and 1 MCF-7 cell were isolated in 6 individual chambers and in 2 chambers no cells were punched and used as negative control.

DNA amplification and validation

The DNA content of a single cell is approximately only 6–7 pg, which is not sufficient for reliable genetic analysis, therefore amplification of DNAs obtained from a single cell is required to obtain enough copies of DNAs for the downstream analysis such as quantitative polymerase chain reaction (qPCR) or sequencing. Isolation of cells of interest in microfluidic reaction chambers was followed by lysis and an

amplification step. Lysis buffer was introduced from one of 5 inlets and pumped into the individual chambers for 100 seconds, resulting in approximately 250 nl, to cover the whole surface of the reaction chamber. After 10 min lysis at 65 °C, the same volume of stop solution was added to the reaction chambers and approximately 300 nl of amplification reagent was pumped into individual chambers for 120 seconds. This reagent volume is approximately 130 times smaller compared to the standard protocol. The calculated maximum chamber volume is 785 nl and the reagent volume can be adjusted using peristaltic pumping. The micro-valve in front of the reaction chamber was closed to contain the single reaction and the reaction chambers were sealed to avoid drying and contamination. The microfluidic device was then placed in a water bath to keep the temperature at 30 °C. After 16 hours 1× TE buffer containing 0.2% Tween-20 was filtered and introduced through one of the inlets and pushed to the chambers individually. Approximately 8 µl of the amplified sample were pipetted out of the each chamber. After sample collection phi29 polymerase was inactivated by increasing the temperature to 65 °C for 10 min according to the standard protocol of the commercial kit. The average amount of amplified DNA was 91.4 ng ($n = 6$) providing an amplification of more than 10 000 fold in the chambers with cells. In the chambers without cells a background of 51.84 ng DNA ($n = 2$) was measured. Previous researches showed that the DNA amplification using phi29 can produce non-specific DNAs when the reaction time is extended.³⁵ To validate the quality of amplified DNA, real-time qPCR targeting 8 genes of interests located in different loci was performed. We purified on-chip amplified DNA using Ampure XP magnetic beads, and 1 µl of the 20 µl sample from each chamber was used for qPCR of single genes. Fig. 5 shows the amplified (green) and non-amplified (white) genes of individual samples of 8 genes positioned at different loci on the chromosomes. A Cq (threshold cycle) value lower than 40 with a correct melt curve was

considered as a positive product. On-chip amplified DNA of 25 cells successfully amplified 8 of 8 genes. Amplified DNA of less than 5 cells detected 3–5 of the 8 genes. These amplified genes can be analysed in more detail using for example sequencing to identify specific alterations. On the other hand, amplified DNA in the chambers without cells did not amplify any of the 8 genes. This verified that the amplified DNA in the negative chambers was a non-specific product. Even though the methods for whole genome amplification of single cells has been improved, amplification bias of amplified DNA from single or few cells still exist. Likely further improvements in the single cell amplification kits are expected and will improve the representation of the genes at low cell numbers. Examples are whole genome amplification of single cells with methods such as adapter-linker PCR³⁶ or multiple annealing and looping-based amplification cycles (MALBAC)³⁷ that already have been developed and demonstrated in the field. Improved amplification kits could be adaptable due to the flexible volume control offered by peristaltic pumping under temperature control. Other causes for the lesser gene representation at low cell numbers could be the drying procedure included in the sample preparation steps. Isolation of single cell in liquid could improve the quality of DNA. Expanding this technology for the future may be able to perform cultivation or drug-response monitoring of cells after isolation of cells in liquid.

Conclusions

Here, we developed a microfluidic device to enrich and isolate individual tumor cells from whole blood and amplify its DNA for further characterization. This was achieved by combining self-seeding microwell chips and open-well reaction chambers connected to fluidic channels. Micro-valves were used to add different reagents in sequence and allow for 8 single reactions. We demonstrated that after seeding of 1 ml of leukocyte depleted whole blood on the microwell chip, individual tumor cells can be deposited in an open-well structure microfluidic device in which the individual tumor cells were lysed and the DNA amplified for further characterization. The combination of the leukocyte depletion and filtration through the 5 µm pores resulted in a carry-over of hundreds of leukocytes and ~37% of MCF-7 cells were recovered and could be discriminated from the leukocytes using EpCAM-PE staining. After identification of the cells of interest they were “punched” into an open-well structure microfluidic device. Peristaltic pumping of micro-valves added reagent to the reaction chambers with precise control of fluid and gave a high flexibility of the reagent volume. Furthermore, open-chambers convey the accessibility of sample after lysis and amplification, allowing the investigation of further genetic information. Validation of amplified DNA was carried out using qPCR targeting 8 different genes of interest. Template-specific genes were only amplified from chambers with MCF-7 cells isolated.

Chambers	1	2	3	4	5	6	7	8	gDNA
# of cells	25	25	5	5	1	1	0	0	
Genes	ERBB2 17q12	■	■	■	■	■	■	■	■
	CCND1 11q13	■	■	■	■	■	■	■	■
	Myc 8q24	■	■	■	■	■	■	■	■
	PRMT2 21q22	■	■	■	■	■	■	■	■
	URB2 1q42	■	■	■	■	■	■	■	■
	P53 17p13	■	■	■	■	■	■	■	■
	TRAM1 8q13	■	■	■	■	■	■	■	■
	PAK1 11q13	■	■	■	■	■	■	■	■

Amplified
 Non-amplified

Fig. 5 Validation of on-chip amplified samples. qPCR targeting 8 genes of interest on different loci were performed using 1 µl of amplified and purified DNA. Amplified genes were represented as green and non-amplified genes were represented as white. 2 ng of isolated and purified genomic DNA was used as positive control.

Acknowledgements

This work is supported by NanoNextNL, a micro and nanotechnology consortium of the Government of the Netherlands and 130 partners.

References

- 1 S. D. Meng, D. Tripathy, S. Shete, R. Ashfaq, B. Haley, S. Perkins, P. Beitsch, A. Khan, D. Euhus, C. Osborne, E. Frenkel, S. Hoover, M. Leitch, E. Clifford, E. Vitetta, L. Morrison, D. Herlyn, L. Terstappen, T. Fleming, T. Fehm, T. Tucker, N. Lane, J. Q. Wang and J. Uhr, *Proc. Natl. Acad. Sci. U. S. A.*, 2004, **101**, 9393–9398.
- 2 N. H. Stoecklein, S. B. Hosch, M. Bezler, F. Stern, C. H. Hartmann, C. Vay, A. Siegmund, P. Scheunemann, P. Schurr, W. T. Knoefel, P. E. Verde, U. Reichelt, A. Erbersdobler, R. Grau, A. Ullrich, J. R. Izbicki and C. A. Klein, *Cancer Cell*, 2008, **13**, 441–453.
- 3 W. Hanna, S. Nofech-Mozes and H. J. Kahn, *Breast J.*, 2007, **13**, 122–129.
- 4 W. M. Hanna, J. Rüschoff, M. Bilous, R. A. Coudry, M. Dowsett, R. Y. Osamura, F. Penault-Llorca, M. van de Vijver and G. Viale, *Mod. Pathol.*, 2014, **27**, 4–18.
- 5 S. T. Ligthart, F.-C. Bidard, C. Decraene, T. Bachelot, S. Delalogue, E. Brain, M. Campone, P. Viens, J.-Y. Pierga and L. W. M. M. Terstappen, *Ann. Oncol.*, 2013, **24**, 1231–1238.
- 6 N. Navin and J. Hicks, *Genome Med.*, 2011, **3**, 31.
- 7 A. M. C. Barradas and L. W. M. M. Terstappen, *Cancers*, 2013, **5**, 1619–1642.
- 8 A. van de Stolpe, K. Pantel, S. Sleijfer, L. W. Terstappen and J. M. J. den Toonder, *Cancer Res.*, 2011, **71**, 5955–5960.
- 9 W. J. Allard and L. W. M. Terstappen, *Clin. Cancer Res.*, 2015, **21**, 1–3.
- 10 E. P. Diamandis, K. Pantel, H. I. Scher, L. Terstappen and E. Lianidou, *Clin. Chem.*, 2011, **57**, 1478–1484.
- 11 F. A. W. Coumans, S. T. Ligthart and L. Terstappen, *Transl. Oncol.*, 2012, **5**, 486–491.
- 12 W. J. Allard, J. Matera, M. C. Miller, M. Repollet, M. C. Connelly, C. Rao, A. G. Tibbe, J. W. Uhr and L. W. Terstappen, *Clin. Cancer Res.*, 2004, **10**, 6897–6904.
- 13 A. H. Talasz, A. A. Powell, D. E. Huber, J. G. Berbee, K. H. Roh, W. Yu, W. Xiao, M. M. Davis, R. F. Pease, M. N. Mindrinos, S. S. Jeffrey and R. W. Davis, *Proc. Natl. Acad. Sci. U. S. A.*, 2009, **106**, 3970–3975.
- 14 F. A. W. Coumans, G. van Dalum, M. Beck and L. W. M. M. Terstappen, *PLoS One*, 2013, **8**, e61770.
- 15 S. L. Stott, C. H. Hsu, D. I. Tsukrov, M. Yu, D. T. Miyamoto, B. A. Waltman, S. M. Rothenberg, A. M. Shah, M. E. Smas, G. K. Korir, F. P. Floyd Jr., A. J. Gilman, J. B. Lord, D. Winokur, S. Springer, D. Irimia, S. Nagrath, L. V. Sequist, R. J. Lee, K. J. Isselbacher, S. Maheswaran, D. A. Haber and M. Toner, *Proc. Natl. Acad. Sci. U. S. A.*, 2010, **107**, 18392–18397.
- 16 S. Nagrath, L. V. Sequist, S. Maheswaran, D. W. Bell, D. Irimia, L. Ulkus, M. R. Smith, E. L. Kwak, S. Digumarthy, A. Muzikansky, P. Ryan, U. J. Balis, R. G. Tompkins, D. A. Haber and M. Toner, *Nature*, 2007, **450**, 1235–1239.
- 17 H. W. Hou, M. E. Warkiani, B. L. Khoo, Z. R. Li, R. A. Soo, D. S.-W. Tan, W.-T. Lim, J. Han, A. A. S. Bhagat and C. T. Lim, *Sci. Rep.*, 2013, **3**, 1259.
- 18 R. T. Krivacic, A. Ladanyi, D. N. Curry, H. B. Hsieh, P. Kuhn, D. E. Bergsrud, J. F. Kepros, T. Barbera, M. Y. Ho, L. B. Chen, R. A. Lerner and R. H. Bruce, *Proc. Natl. Acad. Sci. U. S. A.*, 2004, **101**, 10501–10504.
- 19 S. S. Lee, P. Horvath, S. Pelet, B. Hegemann, L. P. Lee and M. Peter, *Integr. Biol.*, 2012, **4**, 381–390.
- 20 P. Y. Chiou, A. T. Ohta and M. C. Wu, *Nature*, 2005, **436**, 370–372.
- 21 D. Robert, N. Pamme, H. Conjeaud, F. Gazeau, A. Iles and C. Wilhelm, *Lab Chip*, 2011, **11**, 1902.
- 22 H. Kortmann, P. Chasanis, L. M. Blank, J. Franzke, E. Y. Kenig and A. Schmid, *Lab Chip*, 2009, **9**, 576–585.
- 23 A. K. White, M. VanInsberghe, O. I. Petriv, M. Hamidi, D. Sikorski, M. A. Marra, J. Piret, S. Aparicio and C. L. Hansen, *Proc. Natl. Acad. Sci. U. S. A.*, 2011, **108**, 13999–14004.
- 24 Y. Marcy, T. Ishoey, R. S. Lasken, T. B. Stockwell, B. P. Walenz, A. L. Halpern, K. Y. Beeson, S. M. D. Goldberg and S. R. Quake, *PLoS Genet.*, 2007, **3**, e155.
- 25 V. Lecault, A. K. White, A. Singhal and C. L. Hansen, *Curr. Opin. Chem. Biol.*, 2012, **16**, 381–390.
- 26 A. K. White, K. A. Heyries, C. Doolin, M. Vaninsberghe and C. L. Hansen, *Anal. Chem.*, 2013, **85**, 7182–7190.
- 27 J. F. Swennenhuis, A. G. J. Tibbe, M. Stevens, J. van Dalum, H. Duy Tong, M. Katika, C. van Rijn and L. Terstappen, *Lab Chip*, 2015, **15**, 3039–3046.
- 28 M. A. Unger, H. P. Chou, T. Thorsen, A. Scherer and S. R. Quake, *Science*, 2000, **288**, 113–116.
- 29 Y. Yang, J. F. Swennenhuis, H. S. Rho, S. Le Gac and L. W. M. M. Terstappen, *PLoS One*, 2014, **9**, e107958.
- 30 M. Hamon, S. Jambovane, L. Bradley, A. Khademhosseini and J. W. Hong, *Anal. Chem.*, 2013, **85**, 5249–5254.
- 31 J. Goulpeau, D. Trouchet, A. Ajdari and P. Tabeling, *J. Appl. Phys.*, 2005, **98**, 044914.
- 32 T. Thorsen, S. J. Maerkl and S. R. Quake, *Science*, 2002, **298**, 580–584.
- 33 F. A. W. Coumans, G. van Dalum, M. Beck and L. W. M. M. Terstappen, *PLoS One*, 2013, **8**, e61774.
- 34 S. de Wit, G. van Dalum, A. T. M. Lenferink, A. G. J. Tibbe, T. J. N. Hiltermann, H. J. M. Groen, C. J. M. van Rijn and L. W. M. M. Terstappen, *Sci. Rep.*, 2015, **5**, 12270.
- 35 P. C. Blainey and S. R. Quake, *Nucleic Acids Res.*, 2011, **39**, e19.
- 36 C. A. Klein, O. Schmidt-Kittler, J. A. Schardt, K. Pantel, M. R. Speicher and G. Riethmüller, *Proc. Natl. Acad. Sci. U. S. A.*, 1999, **96**, 4494–4499.
- 37 C. Zong, S. Lu, A. R. Chapman and X. S. Xie, *Science*, 2012, **338**, 1622–1626.